Journal of Statistical Physics, Vol. 100, Nos. 1/2, 2000

Fluctuations-Inclusive Approach to Phase Transitions in Binary Mixtures

D. Pini,[1] A. Parola,[2] and L. Reatto[1]

Received September 21, 1999; final November 11, 1999

The hierarchical reference theory of fluids (HRT) is applied to the study of the phase diagram of binary mixtures of simple fluids. This approach implements the renormalization group machinery into a liquid-state theory in order to systematically deal with the effect of long-range correlations which play a crucial role in the onset of criticality and phase separation. The effect of fluctuations is embodied in a partial differential equation (PDE) for the free energy of the mixture. Recently, a robust numerical algorithm has been developed which enabled us to integrate this PDE on a substantial density mesh even at low temperature, when the coexistence region spreads over most of the density–concentration plane.

We have considered a model mixture of spherical particles interacting via a hard-core plus attractive tail potential, and adjusted the particle diameters σ_1, σ_2 and the strengths of the attractive interactions ε_{11}, ε_{22}, ε_{12} so as to mimic mixtures of simple fluids such as argon–krypton or neon–krypton. In the latter case the theory reproduces the occurrence of a minimum in the critical temperature (the so-called critical double point) and of immiscibility at high pressure. We have also studied the phase diagram of a symmetric mixture such that $\sigma_1 = \sigma_2$ and $\varepsilon_{11} = \varepsilon_{22}$ as the ratio $\delta = \varepsilon_{12}/\varepsilon_{11}$ is varied. In particular, we find that, in agreement with the mean-field picture, by decreasing δ, a critical endpoint occurring at equal species concentration is turned into a tricritical point. An interesting feature of the HRT is that, whenever phase coexistence occurs, the conditions of phase equilibria are implemented by the theory itself, without any need of enforcing them *a posteriori*. This allows one to straightforwardly map the phase diagram and the critical lines of the mixture.

KEY WORDS: Binary mixtures; fluctuations; phase diagram; critical points; argon–krypton mixture; neon–krypton mixture; symmetric mixture.

[1] Istituto Nazionale di Fisica della Materia and Dipartimento di Fisica, Università di Milano, Via Celoria 16, 20133 Milan, Italy.

[2] Istituto Nazionale di Fisica della Materia and Dipartimento di Scienze Fisiche, Università dell'Insubria, Via Lucini 3, 22100 Como, Italy.

0022-4715/00/0700-0013$18.00/0

1. INTRODUCTION

The description of thermodynamics, structural properties, and phase diagram of simple fluids with spherically symmetric interactions is perhaps the topic in which liquid-state theory has proved most successfull. When one turns to binary mixtures, however, obtaining a similarly accurate description still appears as an open problem even for simple liquids. Unlike in pure fluids, the phase diagrams of mixtures occurr in several different types,[1] whose shape depends sensitively on the interaction parameters, such as the size of the particles and the potential strengths. When comparing theoretical predictions with experimental data, the discrepancies between the model potentials used in the theory and the real interparticle interactions entail therefore a larger ambiguity than in one-component fluids. This is especially true for the interaction between particles of different species. In model mixtures, the unlike-interaction parameters are often obtained from the knowledge of the correspondent quantities for the pure species via some combination rule like the popular Berthelot one.[1] Still, these prescriptions lack a sound foundation, and in order to reproduce the phase diagrams of real mixtures their use is not much more justifiable than fitting altogether the unlike interaction constant to experimental data.

This sensitiveness to the details of the interactions is of course quite a general feature of mixtures. There are however other difficulties which are more directly related with specific theoretical approaches. In particular, both integral-equation and perturbative theories prove difficult to handle when it comes to predicting the phase diagram. In fact, already for pure fluids these theories present a number of problems in the critical and subcritical region: close to a critical point, they either give a naive description with mean-field or spherical exponents,[2] or they fail to show a critical behavior altogether.[3] In principle, this does not necessarily affect the prediction of the phase boundaries away from the critical region. However, this information has to be extracted by enforcing *a posteriori* the conditions of thermodynamic equilibrium between different phases via a Maxwell construction or an equivalent prescription. For binary mixtures, these problems become even more severe: in particular, performing a Maxwell construction is a very cumbersome operation, especially when, as in the modified hypernetted chain (MHNC) integral equation, the phase envelope contains a region where the theory does not have solutions. In the light of the aforementioned difficulities, it is not surprising that the description of thermodynamics and phase equilibria of binary mixtures largely rests upon semi-empirical equations of state which can be regarded as improved van der Waals approximations.

We believe that a significant step towards the task of getting a reliable microscopic theory of phase equilibria in mixtures is achieved by the use of

the hierarchical reference theory of fluids (HRT).[4, 5] This approach can be considered as a method to include into liquid-state theory a careful description of long-range fluctuations which play such a crucial role in criticality and phase separation. In the HRT the attractive part of the interaction is switched on by gradually incorporating its long-wavelength Fourier components into the Hamiltonian of the fluid, and the Helmholtz free energy which results from this process is determined. For a binary mixture, the evolution of the free energy is described by a non-linear partial differential equation (PDE) in three variables, namely the densities ρ_1, ρ_2 of the components and the parameter Q which governs the inclusion of fluctuations. It has already been shown[4] that the universal properties predicted by the HRT in the critical region can be extracted by studying a simplified form of this PDE along the lines of the renormalization group (RG). The scenario which emerges from this analysis shows a number of interesting features. In particular, it provides a microscopic foundation of the phenomenological approach to critical phenomena in mixtures leading to the so-called Fisher renormalization,[6] as well as an explanation for the strong crossovers found in these systems in terms of a competition beween different fixed points of the RG flow.

In order to obtain the non-universal properties of specific mixtures, it is instead necessary to integrate numerically the full PDE. We have recently accomplished this non-trivial task by developing a robust algorithm, which enables us to get stable results even at low temperature and on a substantial density mesh. In the present paper, we are mainly interested in using the HRT to map the phase diagram of model mixtures. In this respect it is worthwhile noting that the HRT is not affected by the shortcomings that haunt conventional liquid-state theories inside the coexistence region. In fact, the inclusion of long-range fluctuations has the effect of preserving the correct convexity of the free energy on the whole phase space. Whenever phase coexistence occurs, the conditions of equilibrium between different phases involving the pressure and the chemical potentials of the components are implemented by the theory itself, without any need of resorting to a Maxwell construction. This feature clearly appears from the collapse of the isothermal sections of the coexistence region on a line in the pressure-chemical potential plane. Besides its theoretical relevance, it also proves to be very useful, as it enables one to straightforwardly determine the phase diagram and the critical lines of the system in study. By assessing the relative weight of density and concentration fluctuations at a critical point, the order parameter of the transition is also obtained.

We have first focused on mixtures of noble gases, namely the argon–krypton[7] and the neon–krypton[8] mixtures, whose phase diagrams present very different topologies and therefore belong to different types of

the Konynenburg–Scott classification.[1] These have been modelled as Lennard–Jones (LJ) mixtures with suitably chosen diameters and interaction strengths. We find that the agreement with the experimental phase diagram is quite satisfactory. However, the comparison with the experiments should not be taken as a very strict test of the accuracy of the theory both because of the discrepancy between the real interaction and the model potential used, and the somewhat inadequate description of the repulsive part of the potential, which has been mapped into a hard-core one with state-dependent, additive diameters. The latter point is important especially when the phase equilibria extend up to very high pressures, such that the detailed shape of the repulsive contribution of the interaction is deeply probed, as is the case with neon–krypton. For this mixture, the representation of the repulsive forces used here proves to be too naive, leading to a systematic overestimation of the pressure at coexistence.

In order to avoid these difficulties, we have considered also genuine hard-sphere plus tail potential mixtures with additive diameters. In particular, we have applied the HRT to the case in which the diameters σ_1, σ_2 and the interaction strengths ε_{11}, ε_{22} between particles of the same species coincide. In these *symmetric* mixtures the only relevant parameter is the ratio $\delta = \varepsilon_{12}/\varepsilon_{11}$ between the unlike- and the like-particles interactions. While such a system bears little resemblance with mixtures of real liquids, its behavior is instead closely related to that of a number of interesting models such as magnetic systems on a lattice with both ferro- and antiferromagnetic coupling,[9] and magnetic liquids on a continuum,[10] both of which have been the object of important contributions by George Stell. In our investigation of symmetric mixtures we have restricted ourselves to the two "extreme" cases of δ close to (but smaller than) one, and of δ much smaller than one. The change in the topology of the phase diagram agrees with the predictions of mean-field calculations and MC simulations.[11] In particular, we find that, as δ gets smaller, a critical endpoint which occurs at equal species concentration is turned into a tricritical point. A more systematic study of the phase diagram including the region at intermediate δ, at which mean-field theory[11, 12] predicts a number of interesting structures, will be deferred to another publication.

The plan of the present paper is as follows: in Section II the HRT for a binary mixture is reviewed, and the HRT equation for the Helmholtz free energy is cast into a form suitable for numerical integration. The results for the argon–krypton and neon–krypton mixtures are compared with experimental data in Section III, while Section IV reports our findings for the phase diagrams of symmetric mixtures. Finally, in Section V we draw our conclusions.

2. THEORY

We consider a mixture of particles belonging to two different species 1 and 2 interacting via a spherically symmetric potential $v_{ij}(r)$, where the indices $i, j = 1, 2$ refer to the two species. We split the potential into a singular contribution $v_{ij}^{\mathrm{R}}(r)$ accounting for the short-range repulsion between the particles and a longer-ranged, attractive one $w_{ij}(r)$:

$$v_{ij}(r) = v_{ij}^{\mathrm{R}}(r) + w_{ij}(r) \tag{1}$$

We assume that the properties of the system interacting via the repulsive potential $v_{ij}^{\mathrm{R}}(r)$ alone are known, so that it can be taken as the unperturbed or reference system. We then turn on the attractive perturbation $w_{ij}(r)$ by gradually including its long-wavelength Fourier components into the hamiltonian of the system. Specifically, we introduce a parameter Q and a potential $w_{ij}^{Q}(r)$ such that at any given stage only the components of $w_{ij}(r)$ with wavevector $k \geqslant Q$ have been taken into account, while those with $k < Q$ have been suppressed. If we let Q evolve from $Q = \infty$ to $Q = 0$, the reference and the fully interacting systems are then connected by a sequence of *Q-systems* with a potential $v_{ij}^{Q}(r) = v_{ij}^{\mathrm{R}}(r) + w_{ij}^{Q}(r)$, in which fluctuations over lengthscales $L > 1/Q$ are strongly inhibited. Only in the limit $Q \to 0$ do we recover the full attractive interaction and the possibility for the system to develop long-range correlations. The equation governing the evolution of the Helmholtz free energy A_Q of the Q-system along with this process can be determined exactly. We have

$$\frac{\partial \mathscr{A}_Q}{\partial Q} = -\frac{Q^2}{4\pi^2} \log\{\det[\mathbf{1} - \mathscr{C}_Q^{-1}(Q)\, \Phi(Q)]\} \tag{2}$$

Here both $\mathscr{C}_Q^{-1}(k)$ and $\Phi(k)$ are 2×2 symmetric matrices. The elements of $\Phi(k)$ are given by $\Phi_{ij}(k) = -\beta \tilde{w}_{ij}(k)$, where $\beta = 1/(k_{\mathrm{B}} T)$ is the inverse temperature, and $\tilde{w}_{ij}(k)$ is the Fourier transform of $w_{ij}(r)$. $\mathscr{C}_Q^{-1}(k)$ is the inverse of the matrix $\mathscr{C}_Q(k)$ with elements

$$\mathscr{C}_{ij}^{Q}(k) = c_{ij}^{Q}(k) + \Phi_{ij}(k) - \Phi_{ij}^{Q}(k) \tag{3}$$

where $c_{ij}^{Q}(k)$ is the partial direct correlation function of the Q-system in momentum space. The latter is related to the partial structure factor $S_{ij}^{Q}(k)$ by the Ornstein–Zernike equation

$$[c_Q^{-1}(k)]_{ij} = -\sqrt{\rho_i \rho_j}\, S_{ij}^{Q}(k) \tag{4}$$

ρ_i being the number density of the species i. Note that the direct correlation function introduced here differs from the commonly adopted one insomuch

as it includes the ideal gas contribution $-\delta_{ij}/\rho_i$. The quantity $\mathscr{A}_Q$ is related to the Helmholtz free energy A_Q via the expression

$$\mathscr{A}_Q = -\frac{\beta A_Q}{V} + \frac{1}{2}\sum_{i,j=1}^{2} \rho_i \rho_j [\Phi_{ij}(k=0) - \Phi_{ij}^Q(k=0)]$$
$$-\frac{1}{2}\sum_{i=1}^{2} \rho_i \int \frac{d^3\mathbf{k}}{(2\pi)^3} [\Phi_{ii}(k) - \Phi_{ii}^Q(k)] \tag{5}$$

where V is the volume of the system. The "modified" free energy $\mathscr{A}_Q$ and direct correlation function $\mathscr{C}_Q(k)$ have been introduced in order to remove the discontinuity in Q which affects A_Q and $c_Q(k)$ respectively for $Q=0$ and $Q=k$ because of the discontinuity in $\Phi_Q(k)$. For $Q=0$, as well as in the $Q\to 0$ limit, the modified quantities coincide with the free energy and the direct correlation function of the fully interacting system after all the fluctuations have been taken into account. For $Q=\infty$, $\mathscr{A}_Q$ and $\mathscr{C}_Q(k)$ yield instead the free energy and the direct correlation function which would result from treating the attractive interaction $w(r)$ in mean-field approximation. This acts as the initial condition for the introduction of the non-linear effects of the fluctuations described by Eq. (2). Unfortunately, Eq. (2) is not closed as it involves $\mathscr{C}_Q(k)$ at each Q: in fact, it is the first of an infinite hierarchy of equations involving the correlation functions of higher and higher order.[5] In order to get a closed equation, we must provide some expression for $\mathscr{C}_Q(k)$. This will be the source of all the approximations introduced in the theory. Here we have set:

$$\mathscr{C}_{ij}^Q(k) = c_{ij}^{\mathrm{R}}(k) + v_{ij}^Q \Phi_{ij}(k) \tag{6}$$

where $c_{ij}^{\mathrm{R}}(k)$ is the partial direct correlation function of the reference system. This has been taken as a mixture of hard spheres with additive diameters, and $c_{ij}^{\mathrm{R}}(k)$ has been represented by the Verlet–Weis parameterization.[13] The form of the above closure is suggested by the random phase approximation (RPA),[14] which is found from Eq. (3) for $Q=\infty$. Like in the RPA, the direct correlation function given by Eq. (6) is always an analytic function of k. This approximation is usually referred to as the Ornstein–Zernike *ansatz*. It appears to be a reasonable one for three-dimensional systems because of the relatively small deviations of the true direct correlation function from analiticity at the critical point (we recall that at the critical point one has $c(k)\sim k^{2-\eta}$, $k\to 0$, with $\eta \simeq 0.037$ in three dimensions). Again like in the RPA, Eq. (6) does not take into account the requirement that the radial distribution function $g_Q(r)$ should vanish at short distance for every Q as a consequence of the singular repulsion

between the particles. This constraint, usually referred to as *core condition*, will not be considered here not to make the computation too heavy. An Ornstein–Zernike closure satisfying the core condition was implemented within the HRT for a one-component fluid,[15, 16] where it was found to affect the phase diagram only to a modest degree. The parameter v_{ij}^{Q} in Eq. (6) is a state-dependent quantity which is determined in such a way that the compressibility sum rule is satisfied. This relates the partial structure factors at $k=0$ with the partial compressibilities of the mixture, and can be straightforwardly expressed in terms of the modified free energy and direct correlation function:

$$\mathscr{C}_{ij}^{Q}(k=0)=\frac{\partial^2 \mathscr{A}_Q}{\partial \rho_i\, \partial \rho_j} \tag{7}$$

When this constraint is imposed on Eq. (6), we get

$$\mathscr{C}_{ij}^{Q}(k)=c_{ij}^{\mathbf{R}}(k)+\left[\frac{\partial^2 \mathscr{A}_Q}{\partial \rho_i\, \partial \rho_j}-c_{ij}^{\mathbf{R}}(k=0)\right]\varphi_{ij}(k) \tag{8}$$

where we have set $\varphi_{ij}(k)=\Phi_{ij}(k)/\Phi_{ij}(k=0)$. The thermodynamic consistency condition (7) plays a most important role in the closure scheme adopted: in fact, when $\mathscr{C}_{ij}^{Q}(k)$ as given by Eq. (8) is substituted into Eq. (2), a closed, non-linear partial differential equation (PDE) for $\mathscr{A}_Q$ is obtained. This equation, although approximated, preserves the same diagrammatic structure of the full HRT hierarchy[5] and, as mentioned in the Introduction, allows one to recover the RG scaling in the critical region and a convex free energy in the whole phase space. In this respect, the present scheme differs substantially from a RPA or similar procedure, in which the quantity v_{ij} in Eq. (6) is given *a priori* for the fully interacting system. We also note that the form of the direct correlation function adopted here appears to be the simplest one which both enforces the fundamental sum rule (7) and keeps the information about the microscopic interactions that makes the theory predictive as far as the behavior of specific models mixtures is concerned. Such a closure has already proved to be fairly accurate in mapping the phase diagram of a one-component fluid.[16]

We now sketch the procedure followed to cast the PDE resulting from Eq. (2) and Eq. (8) into a form more suitable for numerical integration. Instead of the Helmholtz free energy, we will adopt as unknown function the quantity

$$U=\log\{\det[\mathbf{1}-\mathscr{C}_Q^{-1}(Q)\,\Phi(Q)]\} \tag{9}$$

which appears in the r.h.s. of Eq. (2). By differentiating this equation twice with respect to the densities and by setting $\omega = -Q^2/(4\pi^2)$ we get

$$\frac{\partial}{\partial Q}\left(\frac{\partial^2 \mathscr{A}_Q}{\partial \rho_i \, \partial \rho_j}\right) = \omega \, \frac{\partial^2 U}{\partial \rho_i \, \partial \rho_j} \tag{10}$$

If in Eq. (8) we set $k = Q$ and differentiate with respect to Q, we then obtain

$$\frac{\partial \mathscr{C}_{ij}^{Q}(Q)}{\partial Q} = \omega \, \varphi_{ij}(Q) \, \frac{\partial^2 U}{\partial \rho_i \, \partial \rho_j} + B_{ij} \tag{11}$$

where

$$B_{ij} = \frac{\partial c_{ij}^{\mathbf{R}}(Q)}{\partial Q} + \frac{1}{\varphi_{ij}(Q)} \left[\mathscr{C}_{ij}^{Q}(Q) - c_{ij}^{\mathbf{R}}(Q) \right] \frac{d\varphi_{ij}(Q)}{dQ} \tag{12}$$

Since the matrix $\mathscr{C}_Q(Q)$ is symmetric, it can be diagonalized by a rotation

$$R(\alpha) = \begin{pmatrix} \cos\alpha & \sin\alpha \\ -\sin\alpha & \cos\alpha \end{pmatrix} \tag{13}$$

so that its elements can be expressed by its eigenvalues λ_1, λ_2 and the angle α as

$$\mathscr{C}_{11}^{Q} = \lambda_1 \cos^2\alpha + \lambda_2 \sin^2\alpha \tag{14}$$

$$\mathscr{C}_{12}^{Q} = (\lambda_2 - \lambda_1) \sin\alpha \cos\alpha \tag{15}$$

$$\mathscr{C}_{22}^{Q} = \lambda_1 \sin^2\alpha + \lambda_2 \cos^2\alpha \tag{16}$$

We can then express the l.h.s. of Eq. (11) in terms of the derivatives of λ_1, λ_2, α with respect to Q. The three equations for $\partial \mathscr{C}_{11}^{Q}/\partial Q$, $\partial \mathscr{C}_{12}^{Q}/\partial Q$, $\partial \mathscr{C}_{22}^{Q}/\partial Q$ given by Eq. (11) can thus be rewritten as

$$\Gamma(\lambda_1, \lambda_2, \alpha) \, \frac{\partial}{\partial Q} \begin{pmatrix} \lambda_1 \\ \lambda_2 \\ \alpha \end{pmatrix} = \omega \begin{pmatrix} w_1 \\ w_2 \\ w_3 \end{pmatrix} + \begin{pmatrix} B_{11} \\ B_{12} \\ B_{22} \end{pmatrix} \tag{17}$$

where the vector (w_1, w_2, w_3) has been defined as

$$(w_1, w_2, w_3) = \left(\varphi_{11} \, \frac{\partial^2 U}{\partial \rho_1^2}, \varphi_{12} \, \frac{\partial^2 U}{\partial \rho_1 \, \partial \rho_2}, \varphi_{22} \, \frac{\partial^2 U}{\partial \rho_2^2} \right) \tag{18}$$

and $\Gamma(\lambda_1, \lambda_2, \alpha)$ is a 3×3 matrix whose form is readily determined from Eqs. (14)–(16). Let us now re-write Eq. (9) in terms of λ_1, λ_2, α: By exploiting the identity $\det(1 - X) = \det X - \mathrm{Tr}\, X + 1$ we find

$$e^U = \frac{\det \Phi}{\lambda_1 \lambda_2} - \frac{\psi_{11}}{\lambda_1} - \frac{\psi_{22}}{\lambda_2} + 1 \tag{19}$$

where ψ_{ij} is an element of the matrix $R^T(\alpha)\, \Phi R(\alpha)$, $R^T(\alpha)$ being the transpose of the matrix $R(\alpha)$. If Eq. (19) is differentiated with respect to Q it yields

$$e^U \frac{\partial U}{\partial Q} = v_1 \frac{\partial \lambda_1}{\partial Q} + v_2 \frac{\partial \lambda_2}{\partial Q} + v_3 \frac{\partial \alpha}{\partial Q} + f \tag{20}$$

where v_1, v_2, v_3, f contain λ_1, λ_2, α, Φ, $\partial\Phi/\partial Q$ and are obtained straightforwardly from Eq. (19). We now use Eq. (17) to express the Q-derivatives of λ_1, λ_2, α appearing in Eq. (20) via the quantities w_1, w_2, w_3 defined in Eq. (18). If we set $\mathbf{w} = (w_1, w_2, w_3)$, $\mathbf{v} = (v_1, v_2, v_3)$, $\mathbf{b} = (B_{11}, B_{12}, B_{22})$ we finally get

$$e^U \frac{\partial U}{\partial Q} = \omega\{[\Gamma^T(\lambda_1, \lambda_2, \alpha)]^{-1}\, \mathbf{v}\} \cdot \mathbf{w} + \{[\Gamma^T(\lambda_1, \lambda_2, \alpha)]^{-1}\, \mathbf{v}\} \cdot \mathbf{b} + f \tag{21}$$

where Γ^T is the transpose of the matrix Γ and the dots denote scalar product. Since the vector $\mathbf{w}$ contains the second partial derivatives of U with respect to ρ_1 and ρ_2, the above equation is a PDE for U whose "coefficients" depend on ρ_1, ρ_2, Q both explicitly and implicitly via λ_1, λ_2, α. At any given stage of the evolution in Q, Eq. (21) is used to update U, while Eq. (17) is used to update λ_1, λ_2, α. From these, the updated quantities $\mathbf{b}$ (via Eq. (12)), $\mathbf{v}$, f, Γ and hence the updated coefficients of the PDE are determined, so that the procedure can be iterated. We note that the functions U, λ_1, λ_2, α are not independent, as they are related by Eq. (19). In order to ensure that this constraint is satisfied throughout the evolution, the vector $\mathbf{w}$ of the second partial density derivatives of U which appears in Eq. (17) is determined from U as given by Eq. (21).

A technical problem related with the above scheme emerges whenever the Fourier transform of the attractive interaction vanishes, thereby giving a zero in the denominator of the quantities $\mathbf{B}_{ij}$ defined in Eq. (12). From Eq. (8) we immediately find that B_{ij} can also be expressed as

$$B_{ij} = \frac{\partial c_{ij}^{\mathbf{R}}}{\partial Q}(Q) + \left[\frac{\partial^2 \mathscr{A}_Q}{\partial \rho_i\, \partial \rho_j} - c_{ij}^{\mathbf{R}}(k = 0) \right] \frac{\partial \varphi_{ij}}{\partial Q} \tag{22}$$

which does not show any singularity. In fact, $\mathscr{C}_{ij}^{Q}(Q)$ and $c_{ij}^{R}(Q)$ coincide wherever $\varphi_{ij}(Q)$ vanishes, thereby compensating for the vanishing denominator in Eq. (12). This cancellation is however quite awkward to implement numerically. Instead, we can replace the auxiliary variables λ_1, λ_2, α with the eigenvalues Λ_1, Λ_2 of the hessian matrix of the free energy with elements $\partial^2 \mathscr{A}_Q/(\partial\rho_i\,\partial\rho_j)$, and the angle θ of the rotation which puts it into diagonal form. The relation between $\partial^2 \mathscr{A}_Q/(\partial\rho_i\,\partial\rho_j)$, Λ_1, Λ_2, and θ is clearly the same as that between $\mathscr{C}_{ij}^{Q}(Q)$, λ_1, λ_2, and α in Eqs. (14)–(16). From Eq. (10) we readily obtain

$$\Gamma(\Lambda_1, \Lambda_2, \theta)\frac{\partial}{\partial Q}\begin{pmatrix}\Lambda_1\\ \Lambda_2\\ \theta\end{pmatrix} = \omega\begin{pmatrix}u_1\\ u_2\\ u_3\end{pmatrix} \tag{23}$$

where we have set

$$(u_1, u_2, u_3) = \left(\frac{\partial^2 U}{\partial\rho_1^2}, \frac{\partial^2 U}{\partial\rho_1\,\partial\rho_2}, \frac{\partial^2 U}{\partial\rho_2^2}\right) \tag{24}$$

Eq. (23) can be used instead of Eq. (17) as the set of auxiliary equations in the integration of Eq. (21). From Λ_1, Λ_2, θ the hessian of the free energy and hence B_{11}, B_{12}, B_{22} from Eq. (22) are found. Eq. (8) gives the matrix $\mathscr{C}_Q(Q)$, from which λ_1, λ_2, and α are determined. This in turn enables one to find all the coefficients of Eq. (21). On the other hand, for small Q values such that the quantity $\varphi_{ij}(Q)$ is close to one, it is better to resort to the original evolution equation (17) for λ_1, λ_2, α. In fact, inside the coexistence region both the hessian matrix of $\mathscr{A}_Q$ and the matrix $\mathscr{C}_Q(Q)$ have (at least) one vanishing eigenvalue as $Q \to 0$, say Λ_1 and λ_1. Since λ_1 vanishes exponentially, from Eq. (8) we find that Λ_1 must vanish as a power law in Q, so that the behavior of λ_1 results from a cancellation of much more slowly vanishing quantities. In such a situation roundoff errors would prevent us from reliably determining λ_1. This difficulty does not arise instead with Eq. (17), since in it λ_1 is determined directly.

The integration procedure described above may appear at first unnecessarily cumbersome, but it presents the considerable advantage of yielding a PDE, Eq. (21), of quasi-linear form. In such a PDE the partial derivatives of U appear only as multiplicative factors, and all the nonlinearity is embedded into the "coefficients". For this class of equations a simple and very robust integration algorithm can be used,[17] even though the presence of the "off-diagonal" second-density derivative $\partial^2 U/(\partial\rho_1\,\partial\rho_2)$ in Eq. (21) makes the numerical computations more demanding than in the

pure fluid case. The need of an unconditionally stable algorithm is dictated by the strong divergencies developed by Eq. (21) in the coexistence region.

The integration was started at a suitably large value of $Q = Q_0$, and carried on to smaller and smaller Q's by setting $Q = Q_0 \, e^{-t}$, $t \geqslant 0$. We also set $\xi = \rho_1 \sigma_1^3 + \rho_2 \sigma_2^3$, $x = \rho_1 \sigma_1^3 / \xi$, σ_1 and σ_2 being the diameters of the particles, and used these dimensionless quantities instead of ρ_1 and ρ_2 in the numerical integration by expressing the second derivatives of U with respect to ρ_1 and ρ_2 in terms of the derivatives with respect to x and ξ. The variables x and ξ are defined in the intervals $0 \leqslant x \leqslant 1$, $0 \leqslant \xi \leqslant \xi_{\max}$. The high-density boundary $\xi_{\max}$ was set at $\xi_{\max} = 1$. Eq. (21) must be supplemented with an initial condition for $Q = Q_0$ and four boundaries conditions at $x = 0$, $x = 1$, $\xi = 0$, and $\xi = \xi_{\max}$. Provided Q_0 is large enough, we can use for $\mathscr{C}_{Q_0}(k)$ its expression for $Q = \infty$, when, as stated above, $\mathscr{C}_Q(k)$ assumes the RPA form $\mathscr{C}_{Q=\infty}(k) = c^{\mathrm{R}}(k) + \Phi(k)$. This gives the initial condition for U via Eq. (9). The boundary condition at $\xi = 0$ is easily determined, since in the limit $\xi \to 0$ the matrix $\mathscr{C}_Q^{-1}(k)$ vanishes because of the ideal-gas contribution δ_{ij}/ρ_i in $\mathscr{C}_Q(k)$. Eq. (9) then yields $U(\xi = 0, x) = 0$ for every x. The cases $x = 0$ and $x = 1$ correspond to a pure fluid of particles of species 2 and 1 respectively. Hence in order to find these boundary conditions one has to solve the HRT with the closure (6) for a one-component system. This can be done by specializing to such a case the procedure described above. The boundary condition for $\xi = \xi_{\max}$ is more problematic, since binary mixtures, unlike pure fluids, can exhibit fluid-fluid equilibria even at high density as the concentration is changed.[1, 18] In this situation the RPA, which was already used as a high-density boundary condition in the pure fluid case, would be totally inadequate, as it behaves unphysically in the coexistence region. Instead, we have assumed that at high density, concentration fluctuations are much more important than density ones. This seems to be reasonable, since the compressibility of a fluid becomes very small at high density. We then expect the quantity U, which diverges at coexistence in the limit $Q \to 0$, to be much more sensitive to a small change in x than in ξ. Accordingly, in Eq. (21) we have dropped all the partial derivatives with respect to ξ, and thereby ended up with a PDE for U at high ξ in the two variables Q and x. This has been solved by an algorithm similar to that used for the full PDE (21). Since the boundary conditions at $x = 0$, $x = 1$, and $\xi = \xi_{\max}$ hinge themselves on the solution of PDE's, they also require boundary conditions to be specified at the four corners $(\xi, x) = (0, 0)$, $(0, 1)$, $(\xi_{\max}, 0)$, $(\xi_{\max}, 1)$. Those at $\xi = 0$ and $x = 0, 1$ are just given by $U = 0$, as stated above. Moreover, the two points $(\xi_{\max}, 0)$, $(\xi_{\max}, 1)$ correspond to a pure fluid at high density, for which we do not expect any fluid-fluid phase transition. We can then confidently adopt the RPA $\mathscr{C}_Q(k) = c_{\mathrm{R}}(k) + \Phi(k)$ as a boundary condition at these

points. The numerical integration was performed on a 100×100 grid in the (ξ, x) space, while the variable $t = -\ln(Q/Q_0)$ was discretized using a step $\Delta t = 10^{-3}$. The integration with respect to t was carried on until convergence in the quantity U was achieved outside the coexistence region.

3. RESULTS: MIXTURES OF NOBLE GASES

We have applied the theory described in the previous section to mixture of noble gases. In particular, we have considered a model mixture of spherical particles interacting via a Lennard–Jones (LJ) potential. The splitting of the potential into a repulsive and an attractive part has been performed according to the well-known WCA procedure.[14] The repulsive contribution has then been mapped into a hard-sphere potential with a temperature-dependent diameter $\sigma_{HS}(T)$ determined via Barker's rule.[14] The particle diameters σ_1, σ_2 and the interaction strengths ε_{11}, ε_{22}, ε_{12} have been adjusted so as to mimic an argon–krypton and a neon–krypton mixture. We fixed the diameters and the strengths of the interaction between like species by requiring that the experimental critical temperatures and pressures of the pure components are reproduced by the theory. Although this might appear like an *ad hoc* prescription, it is in fact a reasonable one, since the HRT in its present implementation leads to an accurate prediction for the critical point of the LJ fluid: we find $T_c^{\mathrm{HRT}} = 1.326$, $P_c^{\mathrm{HRT}} = 0.136$ in reduced units, to be compared with the simulation result[19] $T_c = 1.31$, $P_c = 0.126$. If a better representation of the reference system is used, and the core condition is taken into account,[16] the HRT yields $T_c^{\mathrm{HRT}} = 1.329$, $P_c^{\mathrm{HRT}} = 0.135$, very close to the previous determination. In light of these considerations, we can safely assume that matching the theoretical and experimental critical points of the pure components corresponds to correcting for the discrepancies between the model potential used and the interactions in real systems, much more than fixing some intrinsic deficiency of the theory in an *ad hoc* fashion.

There are however other two more problematic points: first, even if one assumes that the particles 1 and 2 are additive, i.e., that the diameter σ_{12} of the interaction between unlike species is given by $\sigma_{12} = (\sigma_1 + \sigma_2)/2$, this condition in general will not be satisfied by the effective hard-sphere mixture into which the reference system is mapped. The relevance of this point, that has been acknowledged since perturbation theory was applied to binary mixtures, lies in the fact that the thermodynamics and, above all, the structural properties of mixtures of non-additive hard spheres are much less ascertained than those of additive systems, especially in the present case of particles with different diameters. Some approximate equations of

state have been reported in the literature[20] but, to our knowledge, no closed-form expression for the correlations has been given, while the direct correlation function of the reference system is needed in order to implement the HRT. A full treatment of the non-additive hard-sphere mixture appears then to be as complicated as avoiding the mapping of the reference system into a hard-sphere mixture altogether, and describing it directly by some integral-equation theory, like for instance the MHNC, as was already done in the one-component case.[16] Here we just determined the LJ diameter σ_{12} *ad hoc*, in such a way that Barker's rule will give a mixture of additive hard spheres. This procedure should not entail severe consequences for the argon–krypton mixture, since the amount of non-additivity due to Barker's recipe is very small in that case. We can instead expect some drawback in neon–krypton, where the non-additivity is more substantial.

The other difficulty is related to the lack of knowledge of the precise value of the interaction strength between unequal species ε_{12}. Determining *a priori* this quantity is difficult, and probably not even worth doing in the present case, since the correspondent interaction cannot be considered very realistic anyway. We then decided to adjust ε_{12} so as to reproduce some feature of the experimental phase diagram of the mixture under study.

For the argon–krypton mixture we set $\sigma_{\mathrm{Ar}} = 3.52$ Å, $\sigma_{\mathrm{Kr}} = 3.77$ Å, $\varepsilon_{\mathrm{Ar-Ar}} = 113.8\,^{\circ}\mathrm{K}$, $\varepsilon_{\mathrm{Kr-Kr}} = 157.9\,^{\circ}\mathrm{K}$ on the basis of the experimental critical temperature and pressure of the pure components,[7] as stated above. The constant $\varepsilon_{\mathrm{Ar-Kr}}$ was adjusted in such a way that the HRT results would reproduce the experimental ones for the isotherm at $T = 177.38\,^{\circ}\mathrm{K}$.[7] This yields the value $\varepsilon_{\mathrm{Ar-Kr}} = 133.5\,^{\circ}\mathrm{K}$, which is very close to that given by the Berthelot rule $\sqrt{\varepsilon_{\mathrm{Ar-Ar}}\,\varepsilon_{\mathrm{Kr-Kr}}} \simeq 134\,^{\circ}\mathrm{K}$. The difference between the diameter $\sigma_{\mathrm{Ar-Kr}}$ determined according to the prescription described above and the mean value of the diameters of the pure species $(\sigma_{\mathrm{Ar}} + \sigma_{\mathrm{Kr}})/2$ is very small, typically below 0.03%. In Fig. 1 the HRT results for the phase diagram in the pressure–concentration plane at four different temperatures are compared with the experimental data.[7] The concentration of krypton reported in the figure is defined as $c = \rho_{\mathrm{Kr}}/(\rho_{\mathrm{Ar}} + \rho_{\mathrm{Kr}})$. The good accuracy of the HRT predictions using the values of $\sigma_{\mathrm{Ar-Kr}}$ and $\varepsilon_{\mathrm{Ar-Kr}}$ just reported indicates that argon–krypton can be considered as a quasi-Lorentz–Berthelot mixture. As it appears from Fig. 1, the topology of the phase diagram is that of the so-called class I,[1] i.e. the critical points of the pure components are connected by a line of critical points. Increasing the concentration of the less volatile component, krypton in this case, has the effect of monotonically raising the critical temperature from that of pure argon to that of pure krypton. We recall that in the isothermal sections of Fig. 1, a critical point corresponds to an extremum in the pressure P on the

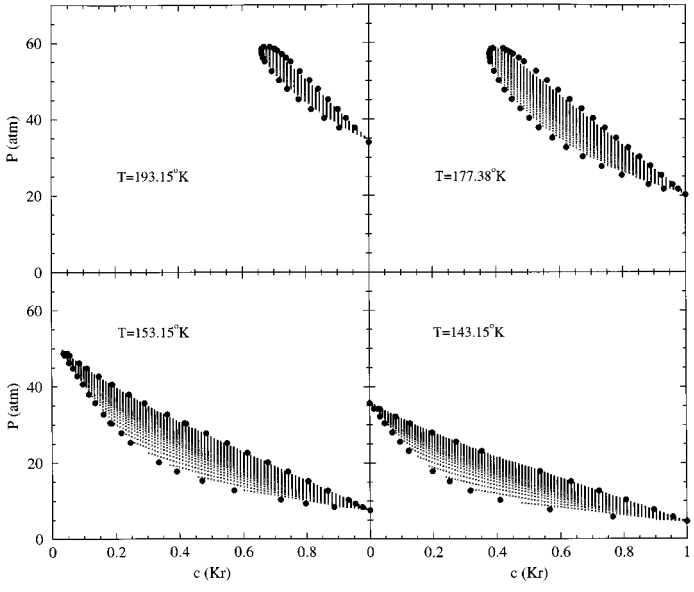

Fig. 1. Isothermal sections of the phase diagram of the argon–krypton mixture in the pressure–concentration plane. c is the molar fraction of krypton. Small squares: HRT two-phase region. Filled circles: experimental results for the phase boundary by Schouten *et al.*[7] The region at $T = 143.15\,^{\circ}\mathrm{K}$ is below the critical temperature of argon and does not have any critical point.

phase boundary such that $(\partial P/\partial c)_{T,\,b} = 0$,[1] the subscript b denoting differentiation along the phase boundary.

We now turn to the neon–krypton mixture. The phase diagram of this system represents another situation commonly found in mixtures, that in which there is no critical line connecting the critical points of the pure components. Instead, a critical line originates from the less volatile component and goes up to higher and higher pressures. In the neon–krypton mixture the temperature does not behave monotonically along this line, but instead has a minimum, so that for temperatures between the minimum and the critical temperature of pure krypton one has both a upper and a lower critical point merging at the minimum into a *critical double point*.[18] At the critical double point a low- and a high-pressure coexistence region coalesce. This is illustrated in Fig. 2, where again the HRT and the experimental results[8] for the phase diagram are compared at four different temperatures. The LJ parameters of neon determined on the basis of the experimental critical point[8] are $\sigma_{\mathrm{Ne}} = 2.85$ Å, $\varepsilon_{\mathrm{Ne-Ne}} = 33.5\,^{\circ}\mathrm{K}$. The strength $\varepsilon_{\mathrm{Ne-Kr}}$ of the neon–krypton interaction has been fixed so as to reproduce the experimental temperature of the critical double point at

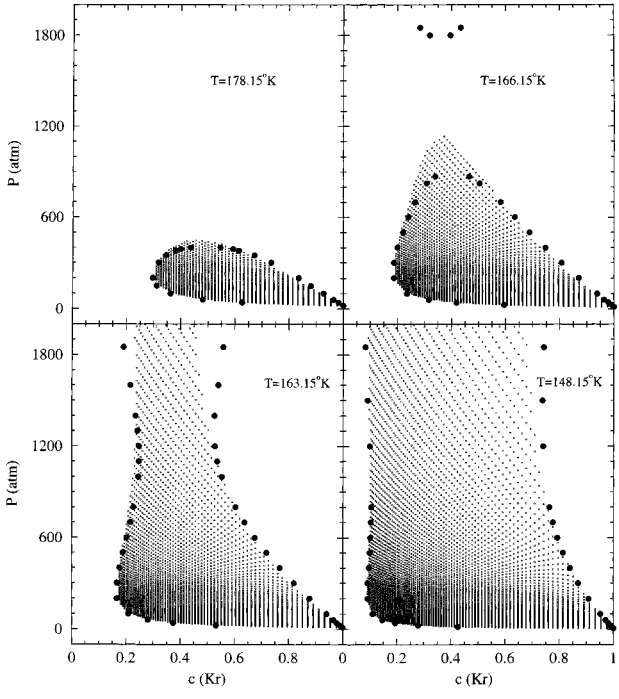

Fig. 2. Isothermal sections of the phase diagram of the neon–krypton mixture in the pressure–concentration plane. Small squares: HRT two-phase region. Filled circles: experimental results for the phase boundary by Trappeniers *et al.*[8] The upper and lower panels correspond to temperatures respectively above and below the critical double point. The high-pressure branch of the HRT coexistence region for $T = 166.15\,^{\circ}\mathrm{K}$ is outside the scale of the figure.

$T = 164.7\,^{\circ}\mathrm{K}$. This gives $\varepsilon_{\mathrm{Ne-Kr}} = 54.3\,^{\circ}\mathrm{K}$. From Fig. 2 it appears that the HRT results, while reproducing the overall shape of the phase diagram, overestimate nevertheless the pressure at coexistence, especially in the high-pressure region. This also results in too high a value of the pressure of the critical double point, which is predicted at about $P \simeq 1900$ atm, while the experimental result is $P = 1240$ atm.[8] Such a discrepancy most probably depends on the fact that the description of the reference system adopted here becomes inadequate for this mixture. We note in this respect that the degree of non-additivity one has to assume in the original interaction in order to end up with a mixture of additive hard-spheres is typically about 1.6%, and is therefore much more substantial than in the argon–krypton case. The unlike interaction strength $\varepsilon_{\mathrm{Ne-Kr}}$ found here is considerably smaller than that given by the Berthelot rule. This is consistent with the

strong non-ideality of the neon–krypton mixture, but the precise value of $\varepsilon_{\mathrm{Ne-Kr}}$ should not be taken too seriously in light of the limitations discussed above. For instance, other investigations based on the Redlich–Kwong equation of state[21] give a $\varepsilon_{\mathrm{Ne-Kr}}$ nearly 20% larger than the above one. It appears then that a more realistic treatment of the repulsive part of the interaction is necessary in order to obtain an accurate description of the high-pressure phase equilibria in this system.

It is worthwhile mentioning that the phase diagrams of both the argon–krypton and the neon–krypton mixtures considered here were determined several years ago via a variational approach using first-order perturbation theory for the Helmholtz free energy and a two-Yukawa tail potential with parameters appropriate to represent a LJ fluid.[22] The variational results appear to be somewhat less accurate than those reported here, especially for argon–krypton, where as the temperature gets close to the critical temperature of krypton the pressure of the phase boundary obtained by the variational theory is overestimated by about 30%. However, this cannot be taken as an assessment of the relative accuracy of the two methods, as in the HRT the LJ interaction parameters have been adjusted on the basis of the experimental phase diagram, while in the variational calculation they were instead determined from experimental second virial coefficients and transport properties.[23] This results in the interaction strengths differing by about 5%. Argon–krypton has also been studied by applying second-order perturbation theory to a hard-sphere plus LJ mixture,[24] where both the hard-sphere diameters σ_{HS} and the LJ diameters and interaction strengths σ, ε were regarded as adjustable parameters. These were fixed by a procedure similar to the one adopted here, namely so as to match the theoretical and experimental critical points of the pure components and of the mixture with relative krypton concentration $c(\mathrm{Kr}) = 0.4$. The critical line is very well reproduced. However, it should be noted that the LJ parameters σ and ε determined by the matching procedure show respectively negative and positive deviations of about 15% from the commonly adopted values,[25] while in HRT the deviations (which go in the opposite directions with respect to those found in perturbation theory) are at most around 5%. This is at least partially due to the higher intrinsic accuracy of HRT in locating the critical point. Second-order perturbation theory has also been applied to binary mixtures of particles with equal-sized, adjustable hard cores plus tail potential which, like the neon–krypton mixture, exhibit high-pressure phase equilibria.[26] This study also shows the sensitiveness of the high-pressure region of the phase diagram to the repulsive potential.

An interesting feature of the HRT is that, as already stated in the Introduction, the conditions of thermodynamic equlibrium between coexisting phases are implemented by the theory itself. More precisely,

whenever phase coexistence occurs, the theory yields a domain in the density–concentration plane, inside which (at least) one eigenvalue of the matrix of the second density derivatives of the Helmholtz free energy is identically zero, i.e. the hessian of the free energy vanishes identically. This implies that, along any isobar inside this region, the chemical potential of each of the two species is constant. Hence such a domain coincides with the coexistence region predicted by the theory. This feature is illustrated in Fig. 3, where four isothermal sections of the phase diagram of the neon–krypton mixture are plotted in the $P-\Delta\mu$ plane, $\Delta\mu$ being the difference between the chemical potentials of the two species. Because of the equilibrium conditions, the coexistence domains collapse into lines, each point of which represents all the points lying on an isobar in the pressure-concentration plane. The critical points are readily found as the points where the coexistence lines in the $P-\Delta\mu$ plane terminate.

The order parameter of the transition is obtained by determining the direction of the strongest fluctuation in the ρ_1, ρ_2 plane. This is given by

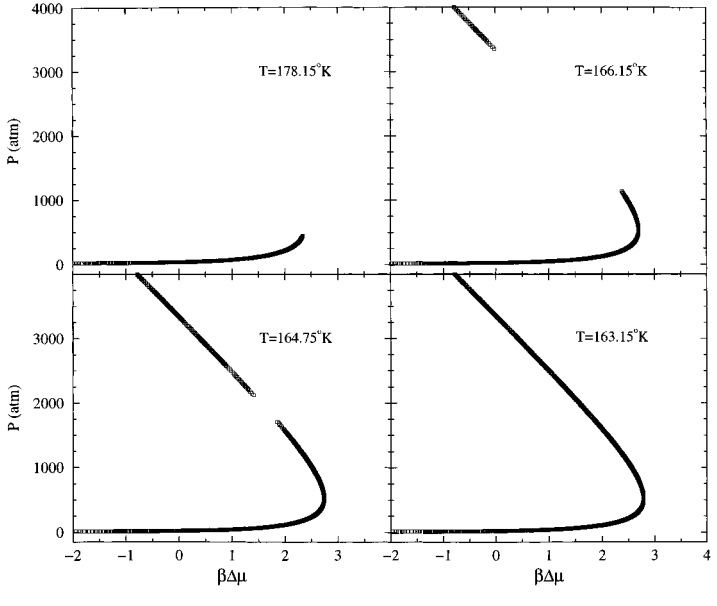

Fig. 3. Isothermal sections of the phase diagram of the neon–krypton mixture in the pressure–chemical potential plane according to the HRT. $\Delta\mu$ is the difference between the chemical potential of neon and that of krypton. The upper and lower critical points merge at the critical dobule point, below which the transition is first order everywhere. Note how the points inside the coexistence region collapse on a line because of the conditions of thermodynamic equilibrium.

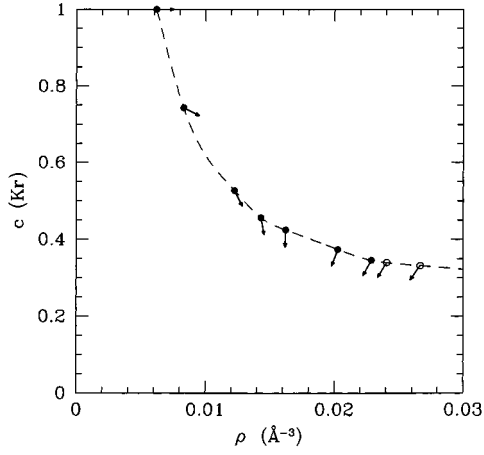

Fig. 4. Critical line of the neon–krypton mixture in the density–concentration plane according to the HRT. The full circles are upper critical points, while the open ones are lower critical points. The arrows indicate the direction of the order parameter. Pure liquid-vapor and mixing-demixing trasitions correspond to the direction parallel to the ρ- and c-axis, respectively. The dashed line is a guide for the eye.

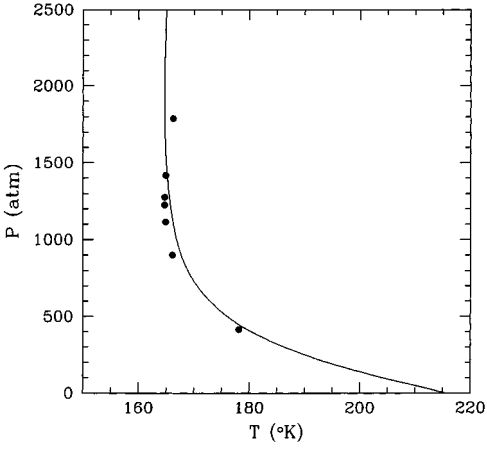

Fig. 5. Critical line of the neon–krypton mixture in the pressure–temperature plane. The critical line originates from the critical point of pure krypton and goes up to higher and higher pressures. The critical double point corresponds to a minimum of the critical temperature. Line: HRT. Filled circles: experimental results.[8]

the linear combination of ρ_1, ρ_2 which corresponds to the vanishing eigenvalue in the hessian of the free energy. By expressing the fluctuations of the order parameter ψ as a function of the fluctuations $\delta\rho$, δc of the total density $\rho = \rho_1 + \rho_2$ and concentration $c = \rho_1/\rho$, one obtains a measure of the dominant character of the transition, either liquid-vapor or mixing-demixing. Fig. 4 shows the projection of the critical line of the neon–krypton mixture given by the HRT in the density–concentration plane. At each critical point, an arrow indicates the direction of the strongest fluctuation. More specifically, the angle ϕ between the arrow and the density axis gives the fluctuation of the order parameter ψ as $\delta\psi = \delta\rho \cos\phi + \rho\, \delta c \sin\phi$. As the neon concentration increases, the transition changes very rapidly from liquid-vapor to mainly mixing-demixing. The HRT critical line is compared to the experimental results in the pressure–temperature plane[8] in Fig. 5. The overall agreement is good, although, as discussed above, the theoretical predictions appear to overestimate the pressure.

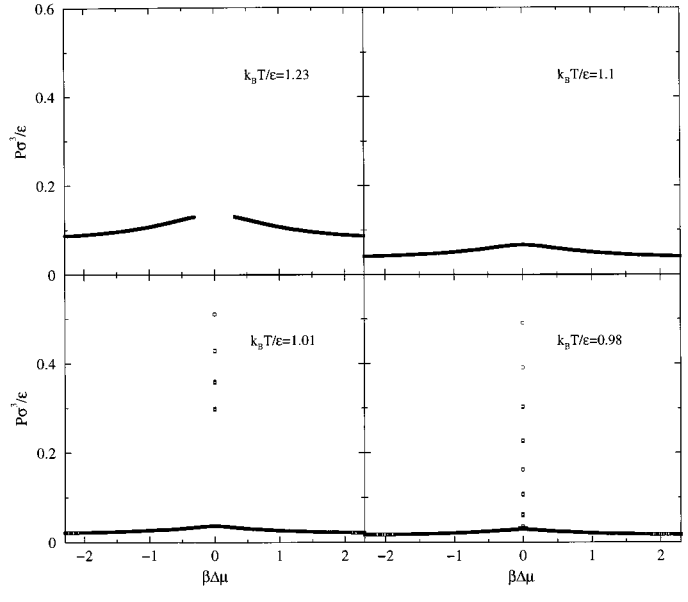

Fig. 6. Coexistence region in the pressure–chemical potential plane of a symmetric hard-sphere plus LJ tail mixture such that $\sigma_1 = \sigma_2 = \sigma$, $\varepsilon_{11} = \varepsilon_{22} = \varepsilon$, $\delta = \varepsilon_{12}/\varepsilon_{11} = 0.8$. $\Delta\mu = 0$ corresponds to equal concentration of the two species. As the temperature is lowered, the mixing-demixing critical point at $\Delta\mu = 0$ meets the low-pressure branch of the coexistence region at a critical endpoint.

4. RESULTS: SYMMETRIC MIXTURES

As stated in the Introduction, a symmetric binary mixture consists of two species 1 and 2 with equal size $\sigma_1 = \sigma_2$ and equal interaction strengths $\varepsilon_{11} = \varepsilon_{22}$ between particles of the same species. The topology of the phase diagram depends on the ratio $\delta = \varepsilon_{12}/\varepsilon_{11}$ between unlike- and like-interaction strengths. Symmetric mixtures have been studied both by mean-field theory[11] and numerical simulations.[11, 27, 28, 29] These studies have been performed either at constant density or at constant concentration, the case of equal species concentration being especially interesting. Here, on the other hand, the whole density–concentration plane will be considered. As usual, we will restrict ourselves to the case $\delta < 1$. In this situation the system presents both a low-density critical line connecting the critical points of the pure components, and a high-density, mixing-demixing one at equal species concentration. As δ is lowered, the mixing-demixing transition becomes more and more favored, and the corresponding critical line moves to lower and lower densities.

We have first considered a symmetric mixture of hard spheres with a LJ tail potential (HSLJ) with $\delta = 0.8$. Fig. 6 shows the coexistence region of this mixture at four different temperatures in the $P - \Delta\mu$ plane. In Fig. 7

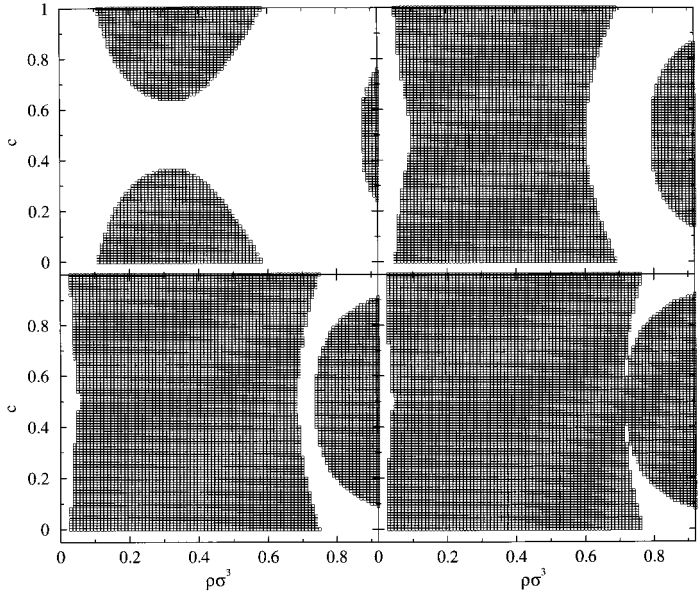

Fig. 7. Same as in Fig. 6 in the density–concentration plane. The temperatures are the same ones reported on the panels of Fig. 6.

the same regions are shown in the density–concentration plane. The high-density coexistence region in Fig. 7 is that associated to the demixing transition, and is represented as a line at $\Delta\mu = 0$ in Fig. 6. This line does not appear in the first two panels of Fig. 6 as it corresponds to very high pressures. Just below the critical temperature of the pure components, two liquid-vapor coexistence regions symmetric with respect to the $\Delta\mu = 0$ or equal concentration axis are also present, each of them ending at a critical point. As T is decreased, these regions coalesce at a critical double point, below which no liquid-vapor critical point is left. The mixing-demixing critical point instead still survives, until it meets the first-order transition boundary of the liquid-vapor coexistence region. The point at which this happens is the *critical endpoint* of the mixing-demixing transition. Below the temperature of the endpoint the transition is first order everywhere. In the case just described the liquid-vapor and the mixing-demixing critical lines are disconnected, with the latter terminating at the endpoint.

For small enough δ a different scenario appears, as shown in Figs. 8, 9, which refer to a HSLJ symmetric mixture with $\delta = 0.5$. At high enough temperature, the only transition is the mixing-demixing one at

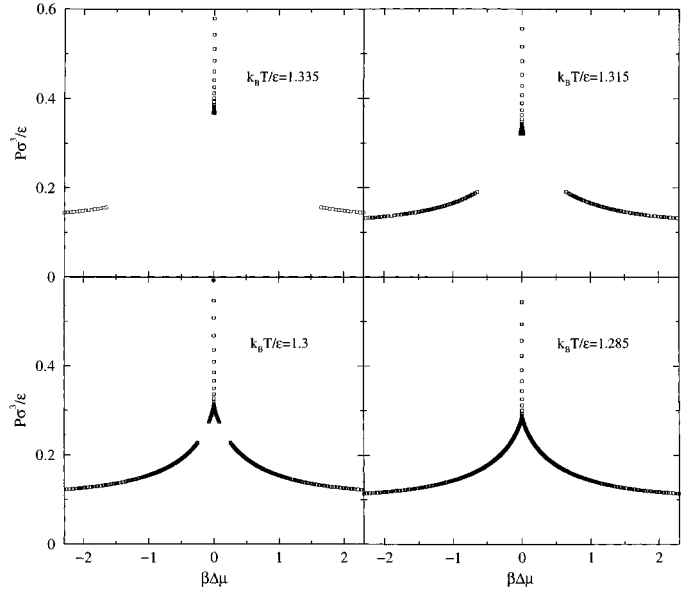

Fig. 8. Same as in Fig. 6 for $\delta = 0.5$. At a temperature $k_B T/\varepsilon = 1.315$ the mixing-demixing critical point at $\Delta\mu = 0$ "bifurcates" into a tricritical point. Below this temperature the point of bifurcation at $\Delta\mu = 0$ is just a first-order phase boundary.

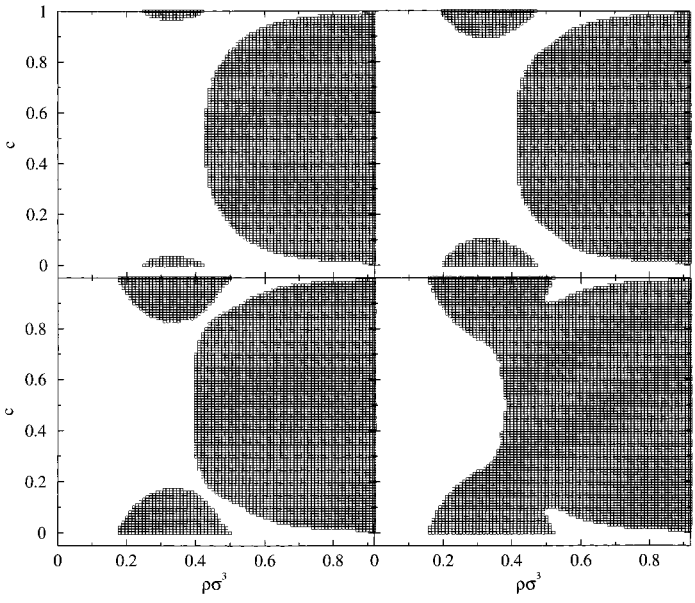

Fig. 9. Same as in Fig. 8 in the density–concentration plane. The temperatures are the same ones reported on the panels of Fig. 8.

$\Delta\mu = 0$, terminating at a mixing-demixing critical point as before. However, below a certain temperature T_t the mixing-demixing coexistence line in the P-$\Delta\mu$ plane terminates in a bifurcation. In this situation there is no critical point at equal species concentration anymore, and the former mixing-demixing critical point becomes a first-order transition point. At exactly $T = T_t$ three critical points meet at a *tricritical point*. We recall that in general a tricritical point does not occurr in binary mixtures.[1] It is found here as a consequence of the special symmetry of the model. As the temperature is further decreased, the low-pressure coexistence regions originating from the critical points of the pure species do not meet each other as before, but instead merge with the high-pressure phase boundary at two distinct critical double points, at which the critical temperature has a minimum. The low-density critical line and the mixing-demixing one are now connected at the tricritical point.

The qualitative description given above is consistent with both mean-field calculations[11, 12] and numerical simulations.[11] It is worthwhile pointing out that for δ values between those corresponding to the two cases presented here, mean-field theory predicts the occurrence of several other topologies for the phase diagram, which we will not discuss here. A more detailed study of this issue will be the subject of further investigation.

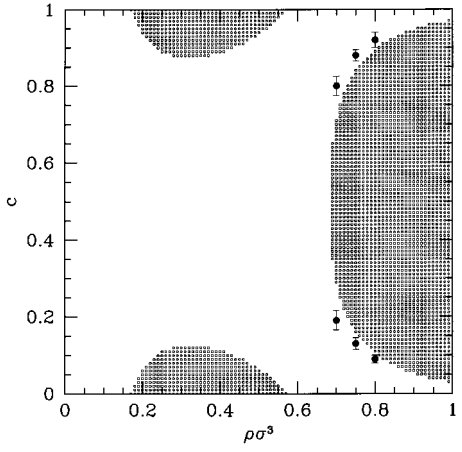

Fig. 10. Coexistence region in the density–concentration plane of a symmetric mixture with a hard-core plus truncated and shifted Yukawa tail potential for $\delta = 0.7$ and $k_B T/\varepsilon = 0.8$. The cutoff radius is $r_{cut} = 3\sigma$ and the inverse screening length is $z = 2.45\,\sigma^{-1}$. Small squares: HRT. Filled circles: semi-grand canonical Monte Carlo results for the phase boundary at constant density $\rho = 0.7,\ 0.75,\ 0.8$.[28]

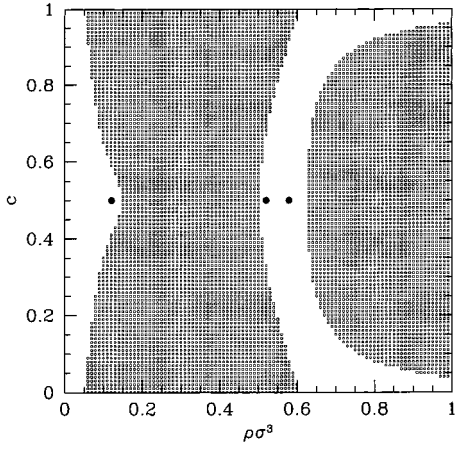

Fig. 11. Coexistence region in the density–concentration plane of a symmetric mixture with a hard-sphere plus square-well potential defined in the interval $\sigma < r < 1.5\sigma$ with $\delta = 0.72$, $k_B T/\varepsilon = 1.03$. Small squares: HRT. Filled circles: finite-size scaling Monte Carlo results for the phase boundary at constant concentration $c = 0.5$ [11].

We conclude this section by comparing our results for the phase diagram of symmetric mixtures with some of the available simulation data. In Fig. 10 the HRT predictions are compared to semi-grand canonical Monte Carlo simulations[28] on a mixture with a hard-core plus Yukawa tail potential $w_{ij}(r) = -\varepsilon_{ij}\sigma \exp[-z(r-\sigma)]/r$, $r > \sigma$, $z = 2.45\,\sigma^{-1}$. The simulations were performed at constant density $\rho = 0.7$, 0.75, 0.8 for $\delta = 0.7$ and $T = 0.8$ in reduced units. In both theory and simulations the Yukawa tail has been truncated at $r_{\text{cut}} = 3\sigma$ and shifted so as to avoid the discontinuity at $r = r_{\text{cut}}$. In Fig. 11 the HRT results are instead compared to finite-size scaling Monte Carlo data[11] at constant concentration $c = 0.5$ for $\delta = 0.72$ and $T = 1.03$. The model potential is a hard-core plus square well $w_{ij}(r) = -\varepsilon_{ij}$, $\sigma < r < 1.5\,\sigma$. It appears that the HRT coexistence regions are somewhat narrower than what indicated by simulations. We recall in this respect that getting a very accurate description of the phase boundaries by simulation is a highly non-trivial task already for pure fluids, and we expect this to be true *a fortiori* for mixtures. Also, on the HRT side, it should be recalled that the RPA-like closure of Eq. (6) does not implement the core condition on the radial distribution function. In the one-component case we found that within the HRT this condition has a negligible influence on the phase diagram, but we do not know whether this should be the case here as well, especially since the phase diagrams of mixtures generally appear to be quite sensitive to the details of the microscopic interactions.

5. CONCLUSIONS

We have applied the HRT with a Ornstein–Zernike closure to binary mixtures of simple fluids. We have considered both mixtures of noble gases such as argon–krypton and neon–krypton, and symmetric mixtures for different relative strengths of the interaction between unlike species. Since in this theory the free energy mantains the correct convexity in the whole thermodynamic space, the phase diagram and the critical lines can be determined straightforwardly. In particular, inside the coexistence region the conditions of phase equilibria are automatically implemented by the theory. This represents a considerable advantage over conventional liquid-state approaches. The accuracy of the results, as assessed by comparison with both experimental and simulation results, is in general very satisfactory, although there is still some room for improvement. In particular, it appears that, in order to accurately describe high-pressure phase equilibria in real systems, one has to carefully take into account the effect of the repulsive part of the potential. The treatment of the reference system provided here, in which the repulsive interaction was first mapped into a

hard-sphere one, and the non-additivity of the hard-sphere mixture entailed by this procedure was then disregarded, proves unsatisfactory at high pressures. A considerable improvement could be obtained by avoiding the mapping of the reference system into a hard-sphere mixture altogether, and describing it via some integral-equation theory like the MHNC. Also, the core condition on the radial distribution function has not been implemented here. This certainly affects the correlations, and could also somewhat affect the thermodynamics. Even at the present stage, this approach appears nevertheless capable of predicting the phase diagram at least as accurately as standard liquid-state theories.

ACKNOWLEDGMENTS

D. P. thanks Dino Costa and Nigel Wilding for helpful correspondence.

REFERENCES

1. See, for instance, J. S. Rowlinson and F. L. Swinton, *Liquids and Liquid Mixtures*, Butterworths, London, 1982.
2. A. Parola and L. Reatto, *Nuovo Cimento D* **6**, 215 (1985).
3. L. Belloni, *J. Chem. Phys.* **98**, 8080 (1993). J. S. Høye, E. Lomba, and G. Stell, *Mol. Phys.* **79**, 523 (1993).
4. A. Parola and L. Reatto, *Phys. Rev. A* **44**, 6600 (1991).
5. A. Parola and L. Reatto, *Adv. Phys.* **44**, 211 (1995).
6. M. E. Fisher, *Phys. Rev.* **176**, 257 (1968).
7. J. A. Schouten, A. Deerenberg, and N. J. Trappeniers, *Physica* **81A**, 151 (1975).
8. N. J. Trappeniers and J. A. Schouten, *Physica* **73**, 546 (1974).
9. C. K. Hall and G. Stell, *Phys. Rev. B* **11**, 224 (1975).
10. E. Lomba, J. J. Weis, N. G. Almarza, F. Bresme, and G. Stell, *Phys. Rev. E* **49**, 5169 (1994). E. Lomba, J. J. Weis, and G. Stell, *Phys. Rev. E* **50**, 3853 (1994).
11. N. B. Wilding, F. Schmid, and P. Nielaba, *Phys. Rev. E* **58**, 2201 (1998).
12. A. Parola, D. Pini, and L. Reatto, unpublished.
13. E. W. Grundke and D. Henderson, *Mol. Phys.* **24**, 269 (1972). L. L. Lee and D. Levesque, *Mol. Phys.* **26**, 1351 (1973).
14. See, for instance, J. P. Hansen and I. R. McDonald, *Theory of Simple Liquids*, Academic Press, London, 1986.
15. A. Meroni, A. Parola, and L. Reatto, *Phys. Rev. A* **42**, 6104 (1990).
16. M. Tau, A. Parola, D. Pini, and L. Reatto, *Phys. Rev. E* **52**, 2644 (1995).
17. W. F. Ames, *Numerical Methods for Partial Differential Equations*, Academic Press, New York, 1977.
18. J. A. Schouten, *Phys. Rep.* **172**, 35 (1989).
19. A. Lotfi, J. Vrabec, and J. Fischer, *Mol. Phys.* **76**, 1319 (1992).
20. H. M. Schaink and C. Hoheisel, *J. Chem. Phys.* **97**, 8561 (1992). E. Z. Hamad, *J. Chem. Phys.* **105**, 3222 (1996). The case of a mixture of non-additive hard spheres with equal diameters has been studied in detail by P. Ballone, G. Pastore, G. Galli, and D. Gazzillo, *Mol. Phys.* **59**, 275 (1986).

21. C. Hoheisel and U. Deiters, *Mol. Phys.* **37**, 95 (1979).
22. S. M. Foiles and N. W. Ashcroft, *J. Chem. Phys.* **75**, 3594 (1981).
23. J. Kestin, S. T. Ro, and W. Wakeham, *Physica* **58**, 165 (1972). J. M. Hellemans, J. Kestin, and S. T. Ro, *Physica* **71**, 1 (1974).
24. G. J. Zarragoicoechea, O. H. Scalise, A. E. Rodríguez, and R. D. Gianotti, *J. Chem. Phys.* **91**, 7130 (1989).
25. I. R. McDonald, *Mol. Phys.* **23**, 41 (1972).
26. G. J. Zarragoicoechea and O. H. Scalise, *J. Chem Phys.* **107**, 4358 (1997).
27. N. B. Wilding, *Phys. Rev. E* **55**, 6624 (1997).
28. C. Caccamo, D. Costa, and G. Pellicane, *J. Chem. Phys.* **109**, (1998).
29. D. G. Green, G. Jackson, E. de Miguel, and L. F. Rull, *J. Chem. Phys.* **101**, 3190 (1994). E. de Miguel, E. M. del Río, and M. M. Telo da Gama, *J. Chem Phys.* **103**, 6188 (1995).